Pattern of Failure in Patients with Biochemical Recurrence After PSMA Radioguided Surgery

Lilit Schweiger[1,2], Tobias Maurer[3,4], Ricarda Simon[4], Thomas Horn[4], Matthias Heck[4], Wolfgang A. Weber[1], Matthias Eiber[1], and Isabel Rauscher[1]

[1]*Department of Nuclear Medicine, School of Medicine, Technical University of Munich, Munich, Germany;* [2]*Department of Nuclear Medicine, Medical University of Innsbruck, Innsbruck, Austria;* [3]*Martini-Klinik and Department of Urology, University Hospital Hamburg-Eppendorf, Hamburg, Germany; and* [4]*Department of Urology, School of Medicine, Technical University of Munich, Munich, Germany*

Prostate-specific membrane antigen (PSMA)–targeted radioguided surgery (RGS) is evolving as a new treatment modality for patients with early biochemical recurrence of prostate cancer and disease limited to locoregional lymph nodes on PSMA-ligand PET/CT. Nevertheless, the pattern of failure (locoregional vs. systemic) after PSMA RGS remains unknown. Therefore, the aim of this retrospective analysis was to evaluate the pattern of disease using PSMA-ligand PET in patients experiencing relapse after PSMA RGS. **Methods:** We evaluated 100 patients with biochemical recurrence after previous PET-guided PSMA RGS who underwent PSMA-ligand PET (median prostate-specific antigen [PSA], 0.9 ng/mL; range, 0.2–14.2 ng/mL). All suspicious lesions for recurrent prostate cancer were grouped according to the molecular imaging TNM classification system. Detection rates and lesion localization were determined and stratified by PSA values and the International Society of Urological Pathology grade group. Further, lesion localization was compared before and after PSMA RGS. **Results:** The median time between PSMA RGS and PSMA-ligand PET for relapse was 11.4 mo (range, 5.5–25.6 mo). In total, 91 of 100 (91%) patients showed PSMA-ligand–positive findings. PSMA PET detection rates were 82.6%, 92.6%, 91.3%, and 96.3% for PSA levels of 0.2–0.49, 0.5–0.99, 1–1.99, and at least 2 ng/mL, respectively. More than half of the patients (53%; 48/91) showed local recurrence or pelvic lymph node metastases only. Extrapelvic lymph node metastases, bone metastases, and visceral metastases were present in 22% (20/91), 16% (15/91), and 9% (8/91) of the patients, respectively. With increasing International Society of Urological Pathology grade group, the percentage of patients with bone and visceral metastases increased, whereas the number of patients with only locoregional disease decreased. **Conclusion:** PSMA-ligand PET is a useful method to detect and localize recurrent disease in patients with biochemical failure after PSMA RGS, with more than half of the patients presenting with locoregional recurrence, offering the potential for a second local therapy (e.g., radiation therapy or repeated surgery).

Key Words: radioguided surgery; biochemical recurrence; prostate cancer; prostate-specific membrane antigen

J Nucl Med 2025; 66:67–72
DOI: 10.2967/jnumed.124.268151

In the last decade, imaging of recurrent prostate cancer (PCa) has changed fundamentally with the introduction of PET targeting the prostate-specific membrane antigen (PSMA) on PCa cells (*1*). Several analyses have confirmed that recurrent PCa lesions (lymph node or soft-tissue metastases) show significant PSMA-ligand uptake and can be visualized even at low prostate-specific antigen (PSA) values and when only a few millimeters are measured (*2–5*). Thus, PSMA PET imaging is the recommended imaging modality for recurrent PCa and has been incorporated in national and international guidelines (*6*).

Traditionally, watchful waiting or initiation of systemic treatment (e.g., androgen deprivation therapy) is suggested in biochemically recurrent (BCR) PCa with evidence of lymph node metastases. However, there is an increasing interest in individualized locally targeted treatment techniques such as targeted salvage radiation therapy or salvage lymph node dissection (SLND). Several studies have shown that SLND can lead to a complete biochemical response in patients with nodal metastases after radical prostatectomy (*7*). To improve these outcomes, PSMA radioguided surgery (RGS) has been introduced using a γ-probe intraoperatively for improved metastatic lesion detection. The first results show that PSMA RGS can delay the commencement of systemic therapies, which have numerous adverse effects and deteriorate the quality of life (*8,9*). As salvage surgery in oligorecurrent PCa currently constitutes an experimental treatment approach, careful patient selection is mandatory based on life expectancy, low PSA values, and a low number of PSMA PET–avid lesions located in the pelvis (*9*).

The clinical outcome of patients undergoing PSMA RGS has already been evaluated (*9–11*). However, so far a pattern of failure (locoregional vs. systemic metastases) in correlation with clinical parameters in patients with recurrence after PSMA RGS has not been systemically analyzed. Therefore, the aim of this retrospective analysis was to determine the localization of recurrence using PSMA-ligand PET in patients developing a biochemical failure after PSMA RGS and especially to compare its localization before and after PSMA RGS.

MATERIALS AND METHODS

Patient Population

In total, 100 PCa patients (median age, 69 y) who presented with a BCR (PSA value, ≥0.2 ng/mL) after PSMA RGS performed in our institution between January 2015 and July 2022 were retrospectively included.

Received May 30, 2024; revision accepted Sep. 9, 2024.
For correspondence or reprints, contact Lilit Schweiger (lilit.schweiger@mri.tum.de).
Published online Sep. 26, 2024.

Detailed patient characteristics are presented in Table 1. PSMA RGS was initially performed for molecular imaging TNM (miTNM) classifications of pelvic node (miN1/2), prostate bed (miTr), and lymph node metastases (miM1a) in 83%, 14%, and 5% of patients (multiple localizations within 1 patient possible), respectively (Table 1).

TABLE 1
Patient Characteristics

Characteristic	Data
Age (y)	69 (64–75)
iPSA (ng/mL)	8.4 (6.2–14.5)
Initial T stage	
≤pT2c	35 (35)
≥pT3a	64 (64)
NA	1 (1)
Initial N stage	
pN0	72 (72)
pN1	23 (23)
pNx	5 (5)
Initial ISUP grade group	
I	3 (3)
II	31 (31)
III	28 (28)
IV	23 (23)
V	15 (15)
Surgical margin status at RP	
R0	73 (73)
R1	19 (19)
NA	8 (8)
Treatment after RP	
No further treatment	40 (40)
Salvage radiotherapy	54 (54)
Salvage lymphadenectomy	2 (2)
Androgen deprivation therapy	4 (4)
PSA at PSMA RGS (ng/mL)	0.87 (0.50–1.79)
PSA nadir after RGS	
<0.2 ng/mL	51 (51)
≥0.2 ng/mL	49 (49)
Localization of recurrence at PSMA-RGS*	
miTR	14 (14)
miN1/2	83 (83)
miM1a	5 (5)
Number of tumor lesions at PSMA RGS	
1	71 (71)
2	18 (18)
>2	11 (11)

*Multiple localizations within 1 patient possible.

iPSA = intact PSA; NA = not available; ISUP = International Society of Urological Pathology; RP = radical prostatectomy.

Qualitative data are number and percentage. Continuous data are median and interquartile range.

All patients gave written informed consent for the procedure. All reported investigations were conducted in accordance with the Declaration of Helsinki and national regulations. The retrospective analysis was approved by the local ethics committee (permit 99/19). The administration of the PSMA ligands complied with The German Medicinal Products Act (AMG §13 2b) and the responsible regulatory body (Government of Oberbayern).

PSMA-Ligand PET and Image Analysis

All patients underwent a PSMA-ligand PET scan at the time of BCR after PSMA RGS. PET/CT was performed in 88 patients, whereas PET/MRI was performed in 12 patients. ^{18}F-rhPSMA-7/7.3, ^{68}Ga-PSMA-11, and ^{18}F-PSMA-1007 were used as PSMA ligands in 64%, 28%, and 8% of patients, respectively.

PSMA-ligand PET/CT was performed on a Biograph mCT flow scanner (Siemens Medical Solutions). A diagnostic CT scan was performed in the portal venous phase 80 s after intravenous injection of contrast agent (Iomeron 300; BIPSO GmbH) followed by the PET scan. All patients received diluted oral contrast (300 mg of Telebrix; Guerbet) and 40 mg of furosemide. All PET scans were acquired in the 3-dimensional mode with an acquisition time of 1.1 mm/s. Emission data were corrected for randoms, dead time, scatter, and attenuation and were reconstructed iteratively by an ordered-subsets expectation maximization algorithm (4 iterations, 8 subsets) followed by a postreconstruction smoothing gaussian filter (5-mm full width at half maximum). Simultaneous PSMA-ligand PET/MRI was performed using an integrated whole-body PET/MRI system (Siemens Biograph mMR; Siemens Healthcare). Details of the protocol and PET data reconstruction were published previously (*12*).

All PET images taken before and after PSMA RGS were reviewed by 1 board-certified nuclear medicine physician. For lesion assessment, the Prostate Cancer Molecular Imaging Standardized Evaluation criteria version 1 were used (*13*). The miTNM classification system is a standardized reporting framework for exact lesion description and organization and may be applied for PSMA-ligand PET/CT as well as for PET/MRI. Hence, all lesions suspected of recurrent PCa were noted and grouped into miTr, miN1/2, miM1a, bone metastases (miM1b), and visceral metastases (miM1c) using the miTNM framework.

Statistical Analysis

Mean values, medians, interquartile ranges, and ranges are presented for quantitative data as appropriate. Lesion localizations were noted and stratified by the International Society of Urological Pathology grade groups (*14*). Detection rates were determined and stratified by PSA values. Lesion localizations were compared on the basis of the highest miTNM score per patient. The change in lesion localization is illustrated using a Sankey diagram. Finally, a descriptive comparison of template-based analysis of pelvic lymph nodes prior to PSMA RGS was performed. Statistical analyses were conducted with MedCalc statistical software (version 13.2.0).

RESULTS

Detection Rates

In total, 91 of 100 patients (91%) showed PSMA-ligand–positive findings in one of the follow-up PSMA-ligand PET scans. The median time between PSMA RGS and a positive PSMA-ligand PET scan for secondary BCR was 11.4 mo (range, 5.5–25.6 mo). The median PSA at the time of PSMA-ligand PET was 0.9 ng/mL (range, 0.2–14.2 ng/mL). PSMA-ligand PET detection rates were 82.6% (19/23), 92.6% (25/27), 91.3% (21/23), and 96.3% (26/27) for PSA levels of 0.2–0.49, 0.5–0.99, 1–1.99, and at least 2 ng/mL, respectively (Supplemental Fig. 1; supplemental materials are available at http://jnm.snmjournals.org).

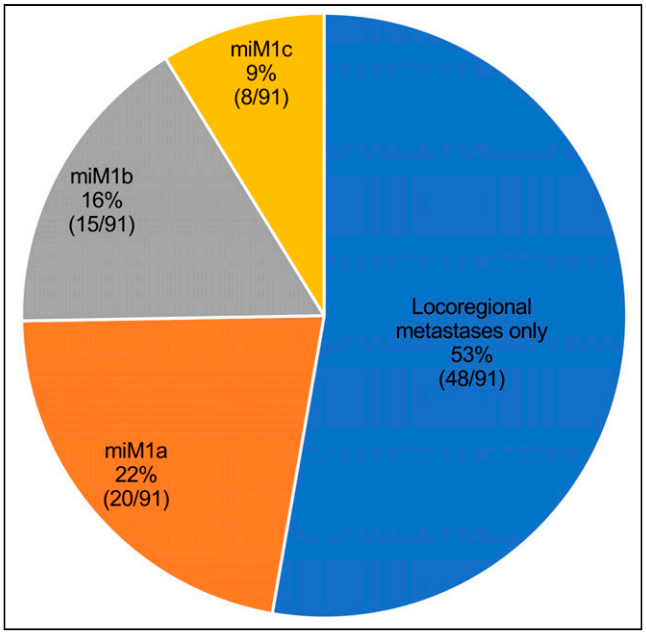

FIGURE 1. Pattern of metastases according to miTNM classification system.

Lesion Localization

More than half of the patients (53%; 48/91) showed local recurrence in miTr or miN1/2 only. Lesions of miM1a, miM1b, and miM1c were present in 22% (20/91), 16% (15/91), and 9% (8/91) of the patients, respectively (Fig. 1). With an increasing International Society of Urological Pathology grade group, the percentage of patients with miM1b increased from 10%, 12%, and 15% for grade groups I + II, III, and IV up to 43% in high-risk grade group V (Fig. 2). In addition, the presence of miM1c metastases increased with a higher International Society of Urological Pathology grade group ranging from 6.5% in grade group I + II to 14.3% in grade group V. In contrast, the number of patients with only locoregional disease decreased from 55%, 69%, and 50% in grade groups I + II, III, and IV to 21% in grade group V (Fig. 2). Interestingly, the percentage of patients with distant miM1a lesions was similar in grade groups I + II, IV, and V (29%, 25%, and 21%, respectively), whereas a slightly lower presence of miM1a lesions was observed in grade group II patients (11.5%).

Comparison of Lesion Localization Before and After PSMA RGS

Lesion localization in PSMA-ligand PET before and after PSMA RGS according to the miTNM classification system is presented in Figure 3. In total, 52.3% (40/76) and 70% (7/10) of initial miN1/2 and miTr patients with a PET scan prior to PSMA RGS showed locoregional metastases (miN1/2 and miTr) again when presenting with BCR after PSMA RGS. miM1a, miM1b, and miM1c disease after PSMA RGS occurred in 21.1% (16/76), 17.1% (13/76), and 9.2% (7/76) of patients with initial miN1 disease and in 0%, (0/10), 20% (2/10), and 10% (1/10) of patients with initial miTr disease prior to PSMA RGS, respectively. Of the 5 patients with miM1a disease prior to PSMA RGS, most (n = 3, 60%) presented with miM1a disease after PSMA RGS, whereas the 2 remaining patients presented with miN1 and miM1b disease.

Supplemental Figure 2 demonstrates detailed, template-based lymph node localization in the pelvis before and after PSMA RGS with multiple localizations within 1 patient. Before PSMA RGS, pararectal lymph nodes (15.8%, 19/120), left iliac internal lymph node (12.5%, 15/120), and local recurrence (11.7%, 14/120) were the most prevalent localizations of metastatic disease, whereas in the BCR after PSMA RGS setting, the most prevalent localization of metastases were local recurrence (16.3, 17/104), retroperitoneal lymph nodes (13.5%, 14/104), and left iliac internal lymph nodes (12.5%, 13/104). Two representative patient examples are presented in Figures 4 and 5.

DISCUSSION

The results of our retrospective analysis demonstrate that only half of the patients (53%) with BCR after PSMA RGS presented with locoregional metastases upon PSMA-ligand PET, whereas

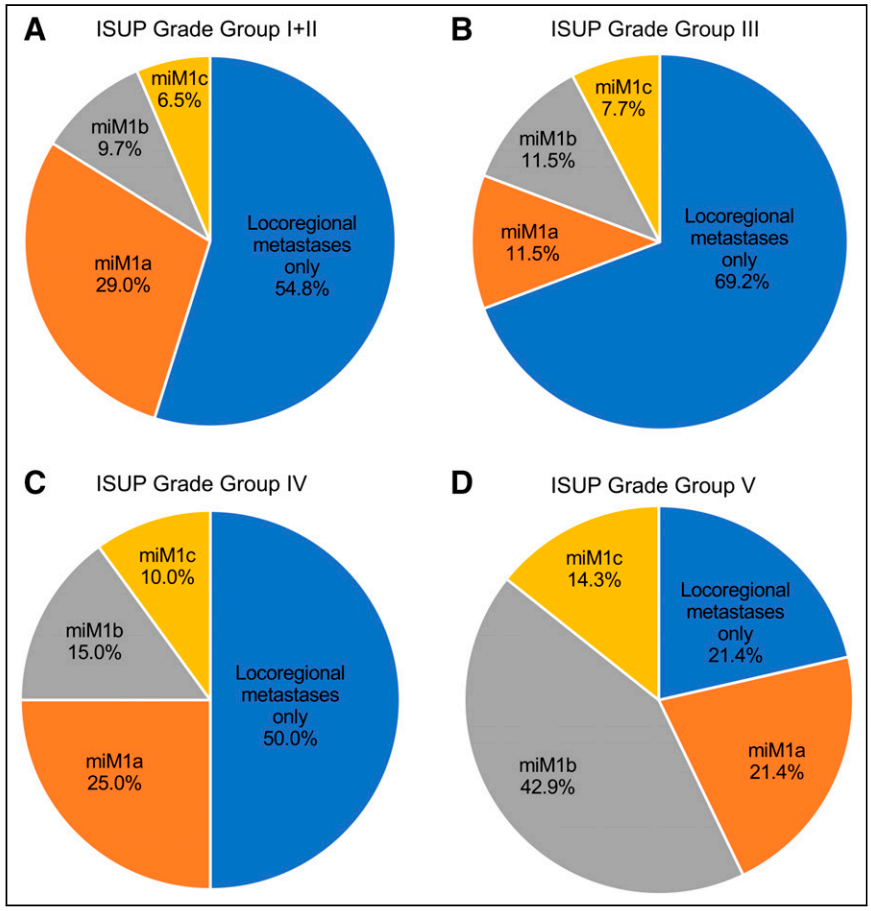

FIGURE 2. Pattern of metastases in International Society of Urological Pathology (ISUP) grade groups I + II (A), III (B), IV (C), and V (D) using miTNM classification system.

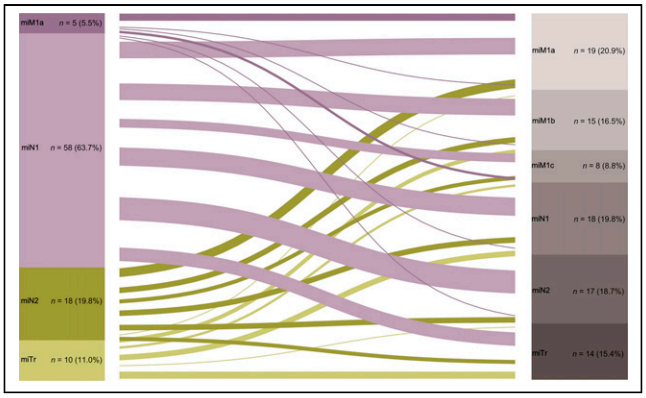

FIGURE 3. Sankey diagram showing change of lesion localization before and after PSMA RGS in patients with positive PSMA-ligand PET scan (n = 91). Only PSMA-ligand PET-positive patients after RGS were included in diagram.

the rest showed distant disease, which not only was limited to lymph nodes (22%) but also progressed to bone (16%) and visceral organs (6%). Consequently, half of the patients would be eligible for a potential second locoregional treatment, underlining the importance of multidisciplinary management of PCa patients, providing imaging specialists, urologists, oncologists, and radiation oncologists the tools to achieve the best possible outcome for PCa patients (*15*).

To the best of our knowledge, this is the first study evaluating the localization of lesions in biochemical failure after RGS. However, multiple studies exist evaluating the pattern of metastases after stereotactic body radiotherapy (SBRT). A study by Ost et al. evaluated the pattern of progression after SBRT for oligometastatic PCa nodal recurrences (*16*). In their analysis, most relapses (68%) occurred in nodal regions, which is in line with our findings in which 65.8% (50/81) of patients with lymph node metastases (miN1/2 and miM1a) relapsed in nodal regions (miN1/2 and miM1a) again. In their study, relapses after pelvic nodal SBRT (n = 36) were most commonly located in the pelvis (n = 14), retroperitoneum (n = 1), pelvis and retroperitoneum (n = 8), or nonnodal regions (n = 13). Another study by Decaestecker et al. assessed the outcome of 50 PCa patients diagnosed with oligometastatic disease at recurrence and treated with SBRT (*17*). For patients with initial pelvic lymph node metastases, 67% of the relapses were located in the pelvic or retroperitoneal nodes and 33% in the bone. Again, these findings match our observations, with 53% of recurrences located in either the prostate bed or pelvic lymph nodes, 21% being located in the extrapelvic region (miM1a), and 18% located in the bone.

Pasqualetti et al. identified the pattern of failure in oligometastasic PCa patients treated with repeated SBRT until disease progression, with 60% of the patients with nodal recurrence experiencing recurrence in a node in close proximity to the previously treated lymph nodes (*18*). Furthermore, most patients with recurrent disease after SBRT relapsed in the same organ system of the initial metastasis (e.g., node–node, bone–bone). This is in accordance with our results in which 52.3% and 70% of the initial miN1/2 and miTr patients undergoing PET prior to PSMA RGS showed locoregional metastases (miN1/2 and MiTr) again when presenting with BCR after PSMA RGS. Further, most patients (60%) with initial miM1a disease experienced recurrence again in extrapelvic lymph nodes (miM1a). However, it is important to note that in our retrospective analysis, the result of the PSMA-ligand PET scan and thus the localization of the newly formed metastases is influenced by the time point of the scan and the median PSA value at the time of the scan. In Figure 5, the patient received a PSMA-ligand PET scan 18 mo after PSMA RGS (with a PSA value of 3.25 ng/mL). The scan showed a clear metastatic progression outside of the pelvis, which may have been different if the scan had been performed at an earlier time point, underlining again the importance of interdisciplinary cooperation for optimal patient management. Despite these limitations, the results of this study are in line with other studies comparing the localization of metastases before and after SLND. Hence, Farolfi et al. compared PSMA-ligand PET before and after SLND in 16 patients with PSA persistence, whereas in our analysis, more than half of the patients (51%) presented with a PSA nadir less than 0.2 ng/mL after PSMA RGS (*19*). In line with our results, disease was confined to the pelvis in 56% of patients, and extrapelvic disease was detected in 31% of patients. However, in study by Farolfi et al., SLND of pelvic nodal metastases was often not complete according to

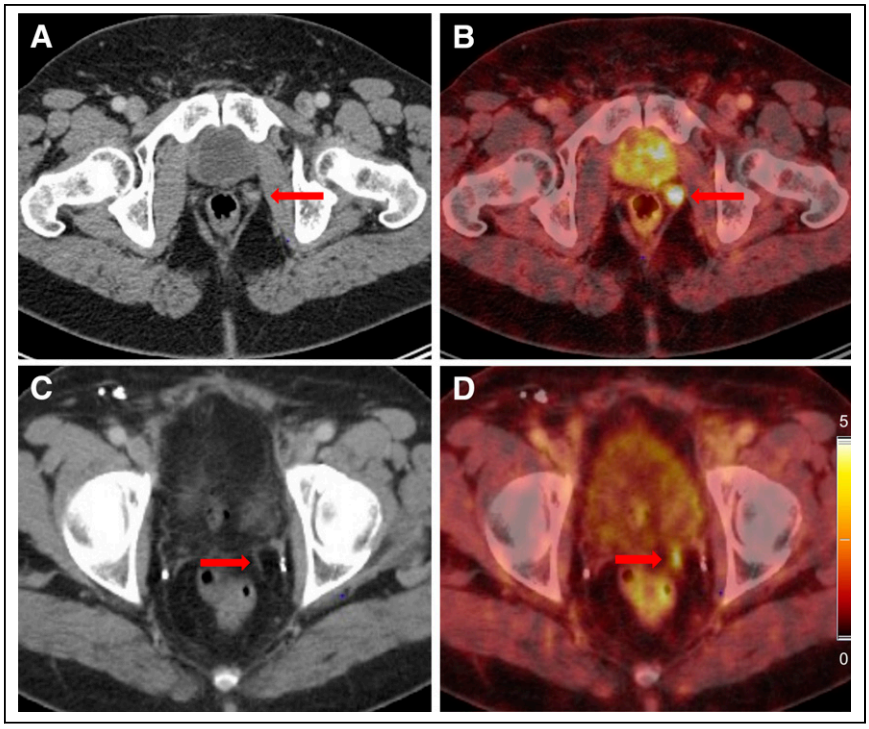

FIGURE 4. 76-y-old patient presenting with local recurrence (arrow) near left seminal vesical bed before PSMA RGS (A and B). PSA level at time of PSMA PET/CT scan was 2.1 ng/mL. PSA nadir after PSMA RGS was 0.29 ng/mL. After RGS, PSA level increased to 0.5 ng/mL. PSMA PET/CT scan after 3 y showed local recurrence in left pelvis (C and D), which was located slightly above initial site of local recurrence.

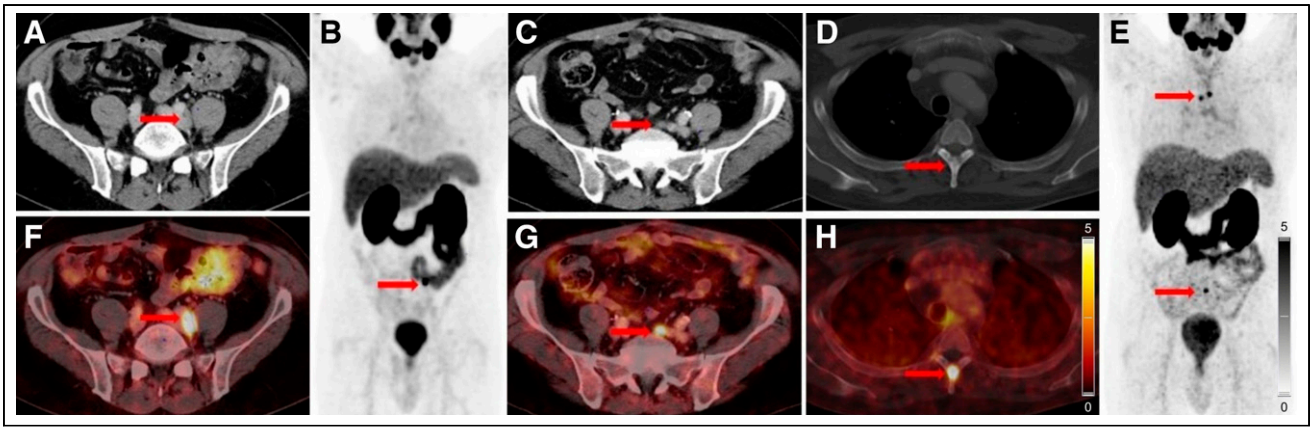

FIGURE 5. 61-y-old patient presenting with BCR with PSA level of 1.35 ng/mL. (A–C) PSMA PET/CT scan showed 2 lymph node metastases adjacent to left common iliac artery (arrows). After RGS, PSA nadir was 0.09 ng/mL, and 18 mo later, PSA level increased to 3.25 ng/mL. (D–H) Second PSMA PET/CT scan showed lymph node metastases adjacent to the left common iliac artery, as well as new bone metastases (T4, fourth rib on left).

PSMA-ligand PET, with about 2 of 3 of patients presenting with PET-positive nodal disease after SLND already seen on the pre-SLND PSMA-ligand PET.

Our retrospective analysis has several limitations. First, a substantial number of patients (49%) in our analysis presented with a PSA nadir of at least 0.2 after PSMA RGS, although PSMA-positive lesions were removed during PSMA RGS. This is most likely related to the fact that even PSMA-ligand PET imaging misses lesions based on the spatial resolution of PET (*2*). Further, it should be emphasized that the study population was scanned with different PSMA ligands (both ^{68}Ga- and ^{18}F-labeled PSMA ligands) and different PET systems (both PET/CT and PET/MR), aspects that might introduce bias and alter the results. Moreover, the time range of patient inclusion was very wide (median time between PSMA RGS and positive PSMA-ligand PET, 11.4 mo; range, 5.5–25.6 mo). Therefore, the time point of the PSMA-ligand PET scan, as well as the PSA value (median PSA, 0.9 ng/mL; range, 0.2–14.2 ng/mL) at the time of the scan varied, potentially impacting the pattern of metastases. As this is an evident bias due to the retrospective nature of the study, further prospective studies with a more structured approach for follow-up imaging are warranted.

CONCLUSION

This retrospective analysis underlines the diagnostic accuracy of PSMA-ligand PET to detect and localize recurrent disease in patients with biochemical failure after PSMA RGS, with more than half of the patients (53%) presenting with local recurrence or pelvic lymph node metastases only. Thus, PSMA-ligand PET could be an accurate method to locate recurrent disease and potentially guide local therapies (e.g., radiation therapy). However, the clinical outcome of additional local therapies in those patients needs to be evaluated in prospective studies.

DISCLOSURE

Isabel Rauscher and Matthias Eiber report fees from Blue Earth Diagnostics Ltd. (consultant, research funding). Further, Matthias Eiber reports fees from Novartis/AAA (consultant, speaker), Telix (consultant), Bayer (consultant, research funding), RayzeBio (consultant), Point Biopharma (consultant), Eckert-Ziegler (speaker), ABX GmbH (speaker), Janssen Pharmaceuticals (consultant, speakers bureau), Parexel (image review), and Bioclinica (image review) outside the submitted work and a patent application for rhPSMA. He and other inventors are entitled to royalties on sales of POSLUMA. No other potential conflict of interest relevant to this article was reported.

KEY POINTS

QUESTION: Where are metastatic lesions in PSMA-ligand PET located in patients developing a second biochemical failure after salvage PSMA RGS?

PERTINENT FINDINGS: In our retrospective analysis of PCa patients with recurrent disease after PSMA RGS, only half of the patients (53%) presented with locoregional metastases in PSMA-ligand PET, whereas the rest showed distant disease, which not only was limited to lymph nodes (22%) but also progressed to bone (16%) and visceral organs (6%).

IMPLICATIONS FOR PATIENT CARE: Our results indicate that more than half of the patients showing locoregional recurrent disease would be eligible for a potential second locoregional treatment (e.g., radiation therapy) and thus could potentially delay the onset of systemic therapies.

REFERENCES

1. Maurer T, Eiber M, Schwaiger M, Gschwend JE. Current use of PSMA-PET in prostate cancer management. *Nat Rev Urol.* 2016;13:226–235.
2. Jilg CA, Drendel V, Rischke HC, et al. Diagnostic accuracy of Ga-68-HBED-CC-PSMA-ligand-PET/CT before salvage lymph node dissection for recurrent prostate cancer. *Theranostics.* 2017;7:1770–1780.
3. Jilg CA, Drendel V, Rischke HC, et al. Detection rate of ^{18}F-choline PET/CT and ^{68}Ga-PSMA-HBED-CC PET/CT for prostate cancer lymph node metastases with direct link from PET to histopathology: dependence on the size of tumor deposits in lymph nodes. *J Nucl Med.* 2019;60:971–977.
4. Rauscher I, Duwel C, Haller B, et al. Efficacy, predictive factors, and prediction nomograms for ^{68}Ga-labeled prostate-specific membrane antigen-ligand positron-emission tomography/computed tomography in early biochemical recurrent prostate cancer after radical prostatectomy. *Eur Urol.* 2018;73:656–661.
5. Perera M, Papa N, Roberts M, et al. Gallium-68 prostate-specific membrane antigen positron emission tomography in advanced prostate cancer-updated diagnostic utility, sensitivity, specificity, and distribution of prostate-specific membrane

antigen-avid lesions: a systematic review and meta-analysis. *Eur Urol.* 2020;77: 403–417.
6. Heidenreich A, Bastian PJ, Bellmunt J, et al. EAU guidelines on prostate cancer. Part II: treatment of advanced, relapsing, and castration-resistant prostate cancer. *Eur Urol.* 2014;65:467–479.
7. Cornford P, Bellmunt J, Bolla M, et al. EAU-ESTRO-SIOG guidelines on prostate cancer. Part II: treatment of relapsing, metastatic, and castration-resistant prostate cancer. *Eur Urol.* 2017;71:630–642.
8. Horn T, Kronke M, Rauscher I, et al. Single lesion on prostate-specific membrane antigen-ligand positron emission tomography and low prostate-specific antigen are prognostic factors for a favorable biochemical response to prostate-specific membrane antigen-targeted radioguided surgery in recurrent prostate cancer. *Eur Urol.* 2019;76:517–523.
9. Knipper S, Mehdi Irai M, Simon R, et al. Cohort study of oligorecurrent prostate cancer patients: oncological outcomes of patients treated with salvage lymph node dissection via prostate-specific membrane antigen-radioguided surgery. *Eur Urol.* 2023;83:62–69.
10. Maurer T, Robu S, Schottelius M, et al. ^{99m}Technetium-based prostate-specific membrane antigen-radioguided surgery in recurrent prostate cancer. *Eur Urol.* 2019;75:659–666.
11. Rauscher I, Eiber M, Maurer T. PSMA-radioguided surgery for salvage lymphadenectomy in recurrent prostate cancer [in German]. *Aktuelle Urol.* 2017; 48:148–152.
12. Souvatzoglou M, Eiber M, Martinez-Moeller A, et al. PET/MR in prostate cancer: technical aspects and potential diagnostic value. *Eur J Nucl Med Mol Imaging.* 2013;40(suppl 1):S79–S88.
13. Eiber M, Herrmann K, Calais J, et al. Prostate cancer molecular imaging standardized evaluation (PROMISE): proposed miTNM classification for the interpretation of PSMA-ligand PET/CT. *J Nucl Med.* 2018;59:469–478.
14. Epstein JI, Egevad L, Amin MB, et al. The 2014 International Society of Urological Pathology (ISUP) consensus conference on gleason grading of prostatic carcinoma: definition of grading patterns and proposal for a new grading system. *Am J Surg Pathol.* 2016;40:244–252.
15. Brausi M, Hoskin P, Andritsch E, et al. ECCO essential requirements for quality cancer care: prostate cancer. *Crit Rev Oncol Hematol.* 2020;148:102861.
16. Ost P, Jereczek-Fossa BA, Van As N, et al. Pattern of progression after stereotactic body radiotherapy for oligometastatic prostate cancer nodal recurrences. *Clin Oncol (R Coll Radiol).* 2016;28:e115–e120.
17. Decaestecker K, De Meerleer G, Lambert B, et al. Repeated stereotactic body radiotherapy for oligometastatic prostate cancer recurrence. *Radiat Oncol.* 2014;9:135.
18. Pasqualetti F, Panichi M, Sainato A, et al. [^{18}F]Choline PET/CT and stereotactic body radiotherapy on treatment decision making of oligometastatic prostate cancer patients: preliminary results. *Radiat Oncol.* 2016;11:9.
19. Farolfi A, Ilhan H, Gafita A, et al. Mapping prostate cancer lesions before and after unsuccessful salvage lymph node dissection using repeat PSMA PET. *J Nucl Med.* 2020;61:1037–1042.